자원환경지질, 제34권, 제6호, 627-648, 2001
Econ. Environ. Geol., 34(6), 627-648, 2001

Origin of Layering and Its Relation to Magma Convection in the Skaergaard Intrusion

Yun D. Jang*

Department of Geological Sciences and Environmental Studies, State University of New York at Binghamton, Binghamton, NY 13902, USA

Skaergaard 암체에서 layering의 기원과 그의 마그마 대류와의 관계

장윤득*

미국 뉴욕주 뉴욕주립대, 지질 및 환경과학과

Skaergaard 암체의 중대에는 사장석 우세대와 휘석 우세대가 교대하는 macro-rhythmic layers와 modally-graded, rhythmic layer를 비롯한 최소 두 가지 종류 이상의 layering이 발견된다. Macro-rhythmic layers는 LS의 중대에서만 빈번히 발견된다. 두께는 0.3에서 3.3 m에 이르고 명확한 상하부 경계를 가지며 노두에서 2 km 이상 횡으로 연장된다. 각기 macro-rhythmic layer에서는 내부적인 점이층리 구조를 보이지는 않으나 소규모 modally-graded layer는 빈번히 발견된다. Modally-graded, rhythmic layer는 LS의 흔히 발견되나 UBS나 MBS에서는 드물게 관찰된다. 두께는 1에서 50 cm에 이르고 노두에서 최대 100 m 까지 횡으로 연속된다. 횡적으로 갑자기 혹은 서서히 사라지며 종종 깍고 메우기 구조나 사층리 구조를 수반한다. 명확한 하부 경계와 점이적인 상부 경계와 함께 강한 층간 modal grading이나 size grading이 특징이다. 중대 modally-graded layering중 사장석 우세와 휘석 우세 macro-rhythmic layer 두개를 상세하게 조사하였다. 일반적으로 사장석 내의 K_2O와 Ba, 휘석, 티탄철석, 그리고 자철석 내의 MgO와 FeO*를 제외한 광물성분변이는 보이지 않는다. 티탄철석과 자철석이 풍부한 layer기저에 산출되는 휘석, 티탄철석, 그리고 자철석의 성분은 MgO가 더 많고 FeO*는 더 적은 경향을 보여준다. 이와 같은 성분변이는 기존의 결정과 Fe가 많은 melt의 상호반응의 결과로 생각되며 Layer 기저에서는 상부보다 적은 re-equilibration를 겪은 것으로 생각된다. 개개 상이나 휘석과 oxide의 비와 reequilibration의 정도 간에는 직접적인 상관관계는 보이지 않는다. 휘석 우세 layer의 사장석에 비해 사장석 우세 layer의 사장석은 UBS의 사장석과 유사하게 상대적으로 적은 K_2O와 Eu/Sm를 보이며 이는 사장석 우세 layer는 암체 상부에서 유래한 과외의 사장석에 기인함을 시사한다. 사장석 우세 layer는 대류기에 휘석 우세 layer는 비대류기에 형성되었음을 시사한다. K2O가 적은 사장석 우세 layer의 사장석은 layer내로 통과하는 K_2O가 풍부한 liquid와의 reequilibration에 기인한 것으로 생각된다. 암체 기저에서 초기에 정출한 것으로 생각되는 K_2O가 많은 휘석 우세 layer의 사장석은 layer내의 interstitial liquid와 평형관계을 이루고 있고 reequilibration의 징후는 보이지 않는다. Modally-graded, rhythmic layer는 Skaergaard 마그마 암장내의 밀도류나 밀도 plume과 암장 기저의 in-situ 결정화작용의 상호작용의 결과로 생각된다.

주요어 : layering, 마그마 대류, 재평형, Skaergaard

At least two distinct types of layering are present in the middle zone of the Skaergaard intrusion; alternating plagioclase-rich and pyroxene-rich, macro-rhythmic layers, and smaller scale, modally-graded, rhythmic layers. The macro-rhythmic layers are ubiquitous in the middle zone of the Layered Series, but are not observed in the lower and upper zone of the Layered Series or in the wall or roof series of the intrusion. They range from 0.3 to 3.3 m in thickness, have sharp upper and lower boundaries, and can be traced laterally for over 2 km in outcrop. Although individual macro-rhythmic layers are not internally graded, many contain smaller-scale, modally-graded layers. Modally-graded, rhythmic layers are a common feature of the Layered Series but are not abundant in either the Upper Border Series or the Marginal Border Series. They range in thickness from 1 to 50 cm and can be traced laterally in outcrop for up to 100 m. Their lateral termination ranges from abrupt to gradational, and they are often associated with cut and fill structures and cross-bedding suggestive of current activity. They are characterized by sharp lower and gradational upper contacts, and by

*Corresponding author: mepark@pknu.ac.kr

strong intra-layer modal grading with olivine, ilmenite, and magnetite concentrated at the base, pyroxene concentrated above the base, and plagioclase concentrated at the top. The layers are also grain-size graded with the maximum size for each phase occurring at the horizon in the layer where the phase is most abundant. Modally-graded, rhythmic layers in the middle zone of the Layered Series occur within both plagioclase-rich and pyroxene-rich macro-rhythmic layers.

Two sequences of modally-graded layering from the Middle Zone have been investigated in detail, one from a plagioclase-rich, macro-rhythmic layer and one from a pyroxene-rich, macro-rhythmic layer. In general, the compositions of individual minerals do not vary systematically within the layers, except for K_2O and Ba in plagioclase, and MgO and FeO* in pyroxene, ilmenite, and magnetite. The compositions of pyroxene, ilmenite, and magnetite are all richer in MgO and poorer in FeO* at the base of layers where ilmenite, and magnetite are abundant. This compositional variation appears to be the result of reaction between early-formed crystals and interstitial Fe-rich melt. Samples at the base of the layers undergo less re-equilibration than samples higher up in the layers suggesting reaction with interstitial melt percolating down through the layer from above. There does not appear to be a direct correlation between the abundance of an individual phase or the pyroxene-oxide ratio and the degree of reequilibration. Compared to plagioclase in the pyroxene-rich layers, plagioclase in the plagioclase-rich layers has lower K_2O contents and lower Eu/Sm, similar to plagioclase in the UBS, suggesting that the plagioclase-rich layers have accumulated excess plagioclase transported from the roof zone of the intrusion. The plagioclase-rich layers may have formed during periods of convection, while the pyroxene-rich layers formed during periods of stagnation. The K_2O-poor plagioclase in the plagioclase-rich layers appears to have reequilibrated with a K_2O-rich liquid percolating downward through the layer. The K_2O-rich plagioclase in the pyroxene-rich macro layers, which is believed to have initially crystallized on the floor of the intrusion, is in equilibrium with the interstitial liquid and shows no reequilibration. Modally-graded, rhythmic layers appear to be the result of interaction between density currents or density plumes and a zone of in-situ crystallization on the floor of the Skaergaard magma chamber.

Key words: layering, magma convection, reequilibration, Skaergaard

1. INTRODUCTION

The Skaergaard is a classic example of a layered intrusion, and a number of different layering types are found within the intrusion. The physical characteristics of the layering suggest that no single mechanism can explain all of the different layering types (Wager and Deer, 1939; Wager and Brown, 1967; Maaloe, 1978; McBirney and Noyes, 1979; Irvine, 1987; Conrad and Naslund, 1989; Naslund and McBirney, 1996; McBirney and Nicolas, 1997; Boudreau and McBirney, 1997; Irvine *et al.*, 1998).

This paper will examine two types of rhythmic layering found in the middle zone of the Skaergaard intrusion. Alternating plagioclase-rich and pyroxene-rich, macrorhythmic layers, and smaller scale modally-graded, rhythmic layers contained within some of the macrorhythmic layers. This paper presents petrographic and geochemical data collected from two representative sequences of modally-graded layering, one sequence from a pyroxene-rich, macro-rhythmic layer and the other sequence from a plagioclase-rich, macro-rhythmic layer.

2. GEOLOGIC SETTING

The Skaergaard intrusion is part of a major igneous province on the east coast of Greenland associated with the opening of the North Atlantic in the Tertiary. The geology of the Skaergaard intrusion was first described by L.R. Wager and his coworkers (Wager and Deer, 1939; Wager and Brown, 1967) who outlined the general field relationships, mineralogical variations, and geochemical trends. Expeditions to the intrusion by later workers added more details about the intrusion and its relationship with regional igneous activities (McBirney, 1989; Naslund, 1984; Hoover, 1989; and numerous others).

The Skaergaard intrusion can be divided into three main units: a Layered Series (LS), which accumulated on the floor of the magma chamber; a Marginal Border Series (MBS), which crystallized along the sides of the chamber; and an Upper Border Series (UBS), which crystallized against the roof of the chamber (Wager and Brown, 1967; Naslund, 1984; Hoover, 1989). The Layered Series is subdivided into lower, middle, and upper zones based on the disappearance and subsequent reap-

pearance of olivine as a primary phase (i.e., the middle zone is generally olivine free). Further divisions of the lower zone into a, b, and c are based on the first appearances of subhedral clinopyroxene and abundant magnetite. The upper zone is similarly subdivided by the first appearances of apatite and ferrobustamite as primary minerals. The subdivisions of the Marginal Border Series and the Upper Border Series are similar to those of the Layered Series, but more compressed. Although their mineral sequences differ in minor ways, the Layered Series, Upper Border Series, and Marginal Border Series all show similar trends of magma differentiation (Naslund, 1984; Hoover, 1989; McBirney, 1989).

3. PETROGRAPHY

Macro-rhythmic layers form a sequence of alternating plagioclase-rich and pyroxene-rich layers in the middle zone of the LS, but are not observed in the wall or roof series of the intrusion. They range from 0.3 to 3.3 m in thickness, have sharp upper and lower boundaries, and are not internally graded. Individual layers are generally of uniform thickness and many can be traced laterally for over 2 km in outcrop. Plagioclase-rich layers, on average, contain more plagioclase (59% vs. 31%), less pyroxene (30% vs. 48%), less opaques (9% vs. 17%), and a higher proportion of ilmenite to magnetite than do pyroxene-rich layers (Naslund *et al.*, 1991).

Modally-graded layers are a widespread, almost ubiquitous feature of the Layered Series of the intrusion from Lower Zone a through Upper Zone a, but are not well developed in the roof or wall sequences. Layers are density-graded with olivine, ilmenite, and magnetite concentrated at the base, pyroxene in the middle, and plagioclase at the top. The lower contacts are sharp but mafic to felsic boundaries within individual layers are generally gradational. They range in thickness from a few centimeters to tens of centimeters and in lateral extent from tens to hundreds of meters. They occur in both plagioclase-rich and pyroxene-rich, macro-rhythmic layers as irregular or random sequences in which individual graded layers are separated by unlayered gabbro. Graded layers are frequently associated with sedimentary-like features such as cross-bedding and scour-and-fill structures. Many layers are laterally graded, becoming more felsic or more mafic along strike before pinching out.

Two representative sequences of modally-graded layering from the middle zone of the Lay-

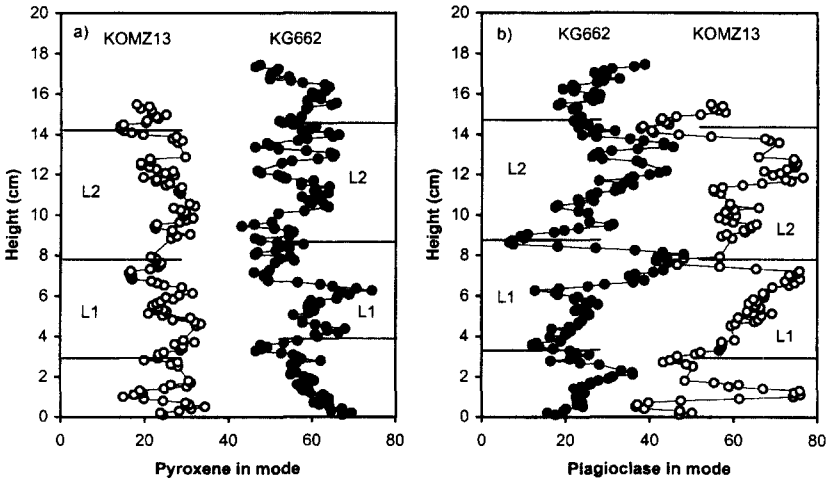

Fig. 1. Plots of modal variation of pyroxene (a) and plagioclase (b) versus height for two representative sequences of macro-rhythmic layers. The macro-rhythmic layers form a sequence of alternating plagioclase-rich and pyroxene-rich layers that contain internal, smaller-scale, modally-graded, rhythmic layers. Note that plagioclase is modally-graded within a layer, but pyroxene, in general, does not show regular interlayer variation. L1 and L2 represent individual layers in each section. Open circles are samples from a 16cm thick sequence in a plagioclase-rich macro layer; filled circles are samples from an 18 cm thick sequence in a pyroxene-rich macro layer, which are most abundant at the base of each layer.

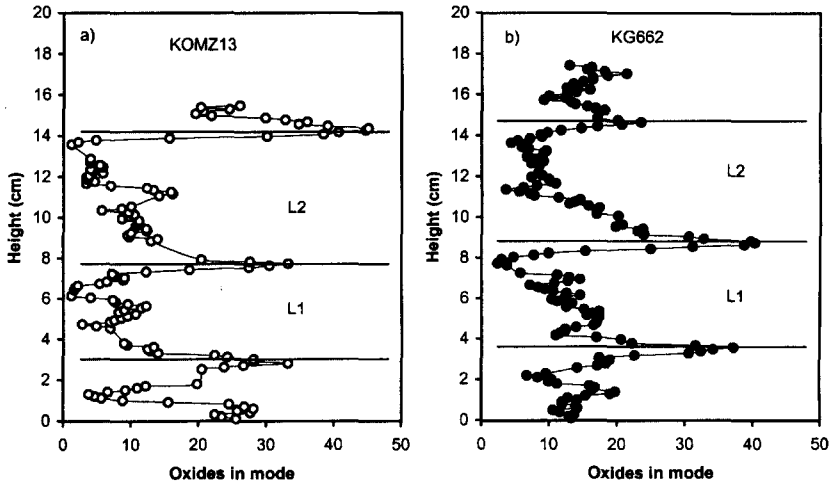

Fig. 2. Plots of modal abundance of opaque minerals versus height for a plagioclase-rich macro layer (a) and a pyroxene-rich macro layer (b). Individual rhythmic layers within the sequences are best defined by the systematic modal variations in opaque minerals.

ered Series have been investigated in detail. One sequence (KG-662) is from a pyroxene-rich, macro-rhythmic layer, and the other sequence (KOMZ-13) is from an adjacent plagioclase-rich, macro-rhythmic layer. Major mineral phases include plagioclase, augite, oxide (generally aggregates of ilmenite and magnetite), and subordinate olivine, which occurs as reaction rims between pyroxene and oxide (Figs. 1 and 2).

Plagioclase is a ubiquitous phase in the Skaergaard intrusion. Within the two sequences studied, the modal abundance of plagioclase varies from 30 to 70% in the plagioclase-rich, macro-rhythmic layer and from 10 to 45% in the pyroxene-rich, macro-rhythmic layer. Plagioclase laths range up to 20mm in length, but are typically 1-5mm (Fig. 3). Significant modal and grain size sorting is observed in plagioclase, with the highest abundances and coarsest grain sizes at the top of each modally-graded layer. Augite is abundant in both of the sequences examined, but Ca-poor pyroxene was not observed in any of these samples. The

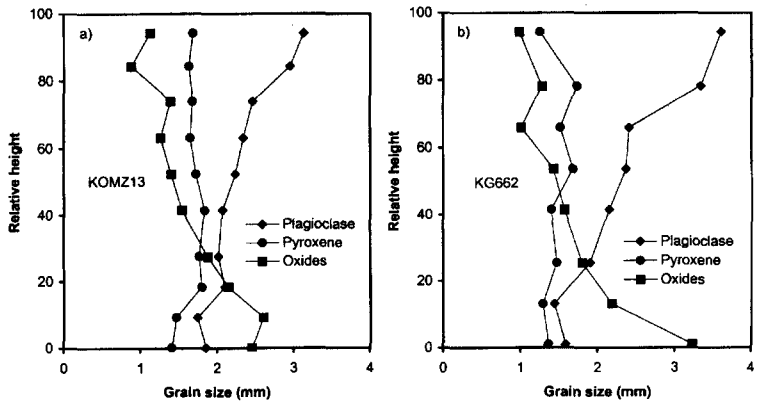

Fig. 3. Grain-size variations in a single modally-graded layer from a plagioclase-rich, modally-graded layer (a) and a pyroxene-rich, modally-graded layer (b). Each point represents an average of 30 to 50 grains. Significant grain size sorting is observed in plagioclase and oxide minerals, with the coarsest grain sizes for each mineral at the level where it has the highest abundances in each modally-graded layer.

modal abundance of augite varies from 10 to 35% in the plagioclase-rich, macro-rhythmic layer and from 45 to 70% in the pyroxene-rich, macro-rhythmic layer. Pyroxene grain sizes range up to 15 mm, but are typically 1-5 mm in length. No primary olivine grains are present in the samples studied. Olivine occurs as reaction rims between pyroxene and oxide, and there is a positive correlation between the presence of olivine and the abundance of oxides. Oxide minerals, which include ilmenite and magnetite-ulvospinel, commonly occur as aggregates of solid solutions that have undergone extensive subsolidus reequilibration and exsolution (Vincent and Phillips, 1954; Vincent, 1960; McBirney, 1989). Grain sizes range up to 15mm, but are typically 1-5 mm across. Owing to the extensive recrystallization, and the aggregate nature of oxide mineral clusters in the samples examined, the measured grain sizes may not represent the initial grain sizes. Modal abundances for combined oxides range from 5 to 40% in both the plagioclase-rich and pyroxene-rich layers. The systematic variation in modal abundance of oxides within the sequences clearly defines the individual rhythmic layers.

4. ANALYTICAL PROCEDURES

Two sequences of modally-graded, rhythmic layers were sampled in the Middle Zone of the Layered Series of the Skaergaard intrusion. One sample (KOMZ13) is representative of plagioclase-rich, modally-graded, rhythmic layers, and the other (KG662) is representative of pyroxene-rich, modally-graded, rhythmic layers. For each sequences 35 thin sections, including 7 thin sections perpendicular to layering and 28 thin sections parallel to layering, were prepared for petrographic and microprobe analysis, and a corresponding set of 28 thin rock slabs were cut for mineral separation and subsequent geochemical analysis. Modal percentages for plagioclase, pyroxene, olivine, and oxides were determined by point counting. Grain sizes (maximum length) of plagioclase, pyroxene, and oxide minerals were measured for between 40 to 70 grains of each mineral phase per sample for one layer from each sequence. Oxide mineral grains are generally made up of aggregates and/or intergrowths of magnetite and ilmenite. I report modal and grain size data for total oxides only, not for magnetite and ilmenite. Fifty six pyroxene and fifty six plagioclase separates were analyzed for this study; twenty eight separates of each were from a sequence of modally-graded, rhythmic layers in a plagioclase-rich macro layer and twenty eight separates of each were from a sequence of modally-graded, rhythmic layers in a pyroxene-rich macro layer. Mineral separation for plagioclase and pyroxene followed conventional procedures using a Frantz isodynamic magnetic separator, heavy liquids of Bromoform and Methylene iodide, and handpicking under a binocular microscope to enhance the purities of mineral separates (cf. Hutchinson 1974). Major and trace element compositions of mineral separates were determined by DCP-AES (Feigenson and Carr, 1985) and ICP-MS in the Department of Geological Sciences at Binghamton University using USGS standards (AGV-1, BCR-1, BHVO-1, DNC-1, GSP-1, and STM-1) for calibration (Govindaraju, 1994). Magnetite and ilme-nite were analyzed using a JEOL 8900 electron microprobe in the Department of Geological Sciences at Binghamton University. Operating conditions were 15 kv accelerating voltage, 15 nA sample current, and 1-3 micrometers beam diameter. The Bence-Albee method (1968) was used for ZAF matrix corrections.

5. MAJOR ELEMENT GEOCHMISTRY

5.1. Pyroxene

In general, pyroxene separates from the two analyzed sequences are similar in major element contents except for MgO and FeO* (total iron as FeO*) (Table 1). Pyroxene in the pyroxene-rich layered sequence is higher in MgO and lower in FeO* than pyroxene in the plagioclase-rich layered sequence. Variations within individual layers are similar in the two sequences. MgO and Mg# (Mg/(Mg+Fe)) in pyroxene progressively decre-ases, and FeO* progressively increases with height in each modally graded layer (Fig. 4). The other major elements do not change systematically with height.

5.2. Plagioclase

In general, plagioclases in the two sequences are similar in composition, except for their K_2O con-

Table 1. Major element analyses of pyroxene separates from two sequences of modally-graded rhythmic layers of the Skaergaard intrusion.

KOMZ13-Plagioclase-rich, modally-graded, rhythmic layer

	Height (cm)	SiO_2	TiO_2	Al_2O_3	FeO*	MnO	MgO	CaO	Na_2O	K_2O	P_2O_5	Total
A1	0.3	49.74	0.76	3.01	15.77	0.36	13.75	16.26	0.14	<0.01	0.03	99.83
A2	0.8	49.81	0.75	2.94	16.08	0.37	13.75	16.12	0.09	<0.01	0.04	99.97
A3	1.3	49.55	0.75	3.09	15.79	0.37	13.53	16.68	0.12	<0.01	0.04	99.93
A4	1.8	49.60	0.75	2.85	15.85	0.38	13.72	16.58	0.12	<0.01	0.04	99.90
B1	2.5	50.24	0.73	2.55	15.39	0.36	13.66	16.19	0.12	<0.01	0.04	99.29
B2	2.9	50.50	0.73	2.60	15.52	0.38	13.78	16.38	0.10	<0.01	0.04	100.04
B3	3.4	50.11	0.73	2.69	15.66	0.38	13.51	16.57	0.10	<0.01	0.04	99.82
B4	3.9	50.05	0.75	2.54	16.06	0.38	13.32	17.00	0.09	<0.01	0.04	100.26
C1	4.6	50.42	0.74	2.60	15.87	0.36	13.18	15.95	0.12	<0.01	0.03	99.28
C2	5.2	50.49	0.75	2.56	16.23	0.38	13.15	15.86	0.10	<0.01	0.04	99.58
C3	5.7	50.96	0.76	2.59	16.24	0.38	13.09	16.34	0.15	<0.01	0.04	100.56
C4	6.3	50.61	0.77	2.47	16.43	0.39	13.06	16.16	0.11	<0.01	0.04	100.05
D1	6.8	50.15	0.77	2.63	16.96	0.38	12.95	16.45	0.11	<0.01	0.04	100.46
D2	7.3	50.09	0.76	2.73	16.59	0.39	13.01	16.23	0.11	<0.01	0.05	99.97
D3	7.9	49.92	0.75	2.68	16.18	0.38	13.67	16.80	0.10	<0.01	0.04	100.53
D4	8.4	49.80	0.76	2.58	16.21	0.38	13.46	16.81	0.13	<0.01	0.05	100.19
E1	9.1	50.11	0.74	2.62	16.33	0.38	13.36	15.66	0.10	<0.01	0.04	99.35
E2	9.7	49.78	0.75	2.65	16.39	0.39	13.24	16.29	0.14	<0.01	0.04	99.68
E3	10.3	50.12	0.76	2.53	16.43	0.38	13.14	16.43	0.12	<0.01	0.04	99.97
E4	10.9	50.03	0.78	2.53	16.50	0.39	13.14	16.50	0.12	<0.01	0.05	100.04
F1	11.6	50.36	0.74	2.51	16.43	0.37	12.92	16.04	0.14	<0.01	0.04	99.55
F2	12.2	50.71	0.75	2.50	16.46	0.38	12.95	15.77	0.12	<0.01	0.04	99.70
F3	12.7	50.57	0.75	2.43	16.59	0.39	12.91	15.77	0.13	<0.01	0.04	99.57
F4	13.3	50.35	0.76	2.48	16.56	0.38	12.78	15.99	0.14	<0.01	0.04	99.49
G1	14.1	50.24	0.74	2.86	16.22	0.37	12.88	15.87	0.15	<0.01	0.04	99.37
G2	14.7	49.88	0.72	2.83	15.66	0.37	13.79	16.31	0.10	<0.01	0.04	99.72
G3	15.3	50.54	0.73	2.73	15.57	0.36	13.60	16.69	0.13	<0.01	0.04	100.42
G4	15.9	50.17	0.74	2.78	15.71	0.37	13.61	16.46	0.14	<0.01	0.04	100.03

FeO*=total iron as FeO

KG662-Pyroxene-rich, modally-graded, rhythmic layer

	Height (cm)	SiO_2	TiO_2	Al_2O_3	FeO*	MnO	MgO	CaO	Na_2O	K_2O	P_2O_5	Total
A1	0.3	50.41	0.73	2.47	16.00	0.37	13.58	16.16	0.19	<0.01	0.04	99.96
A2	0.9	49.98	0.77	2.78	16.27	0.40	13.60	16.39	0.14	<0.01	0.05	100.38
A3	1.4	50.21	0.78	2.42	16.14	0.41	13.72	16.30	0.10	<0.01	0.05	100.14
A4	2.0	50.14	0.76	2.68	16.23	0.41	13.65	16.61	0.05	<0.01	0.05	100.59
B1	2.8	50.23	0.72	2.63	15.66	0.36	13.63	16.06	0.10	<0.01	0.04	99.45
B2	3.3	50.26	0.71	2.40	15.56	0.37	13.78	16.42	0.07	<0.01	0.04	99.61
B3	3.9	50.23	0.75	2.52	15.72	0.37	13.71	16.07	0.09	<0.01	0.04	99.51
B4	4.5	50.19	0.76	2.32	15.99	0.38	13.65	16.21	0.13	<0.01	0.04	99.68
C1	5.3	50.77	0.74	2.33	15.99	0.38	13.53	15.76	0.11	<0.01	0.04	99.64
C2	5.8	50.71	0.78	2.28	16.19	0.38	13.63	15.94	0.12	<0.01	0.05	100.09
C3	6.4	50.28	0.76	2.34	16.21	0.38	13.55	15.99	0.05	<0.01	0.04	99.61
C4	7.0	50.72	0.78	2.30	16.30	0.38	13.55	16.15	0.06	<0.01	0.04	100.28
D1	7.7	50.68	0.78	2.19	16.37	0.37	13.44	15.87	0.11	<0.01	0.04	99.86
D2	8.3	50.79	0.76	1.91	15.92	0.37	13.78	16.08	0.07	<0.01	0.04	99.75
D3	8.9	50.89	0.71	1.94	15.78	0.38	13.76	16.00	0.04	<0.01	0.04	99.54
D4	9.5	50.74	0.75	2.15	15.56	0.37	13.72	15.94	0.09	<0.01	0.04	99.37

Table 1. continued.

	Height (cm)	SiO_2	TiO_2	Al_2O_3	FeO*	MnO	MgO	CaO	Na_2O	K_2O	P_2O_5	Total
E1	10.2	50.71	0.74	2.68	15.52	0.37	13.57	15.75	0.19	<0.01	0.04	99.58
E2	10.8	50.67	0.75	2.45	15.75	0.38	13.57	15.82	0.15	<0.01	0.04	99.59
E3	11.4	50.72	0.74	2.19	16.07	0.38	13.47	15.92	0.09	<0.01	0.04	99.65
E4	12.0	50.79	0.77	2.13	16.23	0.37	13.51	16.20	0.12	<0.01	0.04	100.18
F1	12.8	50.75	0.70	2.53	16.22	0.38	13.38	15.77	0.14	<0.01	0.04	99.92
F2	13.4	50.75	0.75	2.47	16.59	0.39	13.70	15.66	0.11	<0.01	0.05	100.47
F3	14.0	50.84	0.70	2.60	16.36	0.39	13.83	15.55	0.09	<0.01	0.04	100.41
F4	14.6	50.83	0.68	2.81	15.44	0.38	13.88	15.49	0.17	<0.01	0.04	99.73
G1	15.4	50.81	0.73	2.03	15.77	0.37	13.67	15.93	0.21	<0.01	0.04	99.58
G2	16.0	50.82	0.76	2.35	15.82	0.38	13.73	15.96	0.15	<0.01	0.05	100.02
G3	16.6	50.82	0.71	2.03	15.80	0.39	13.94	15.97	0.10	<0.01	0.05	99.83
G4	17.2	50.84	0.74	1.95	15.81	0.39	13.91	15.77	0.13	<0.01	0.05	99.60

FeO*=total iron as FeO

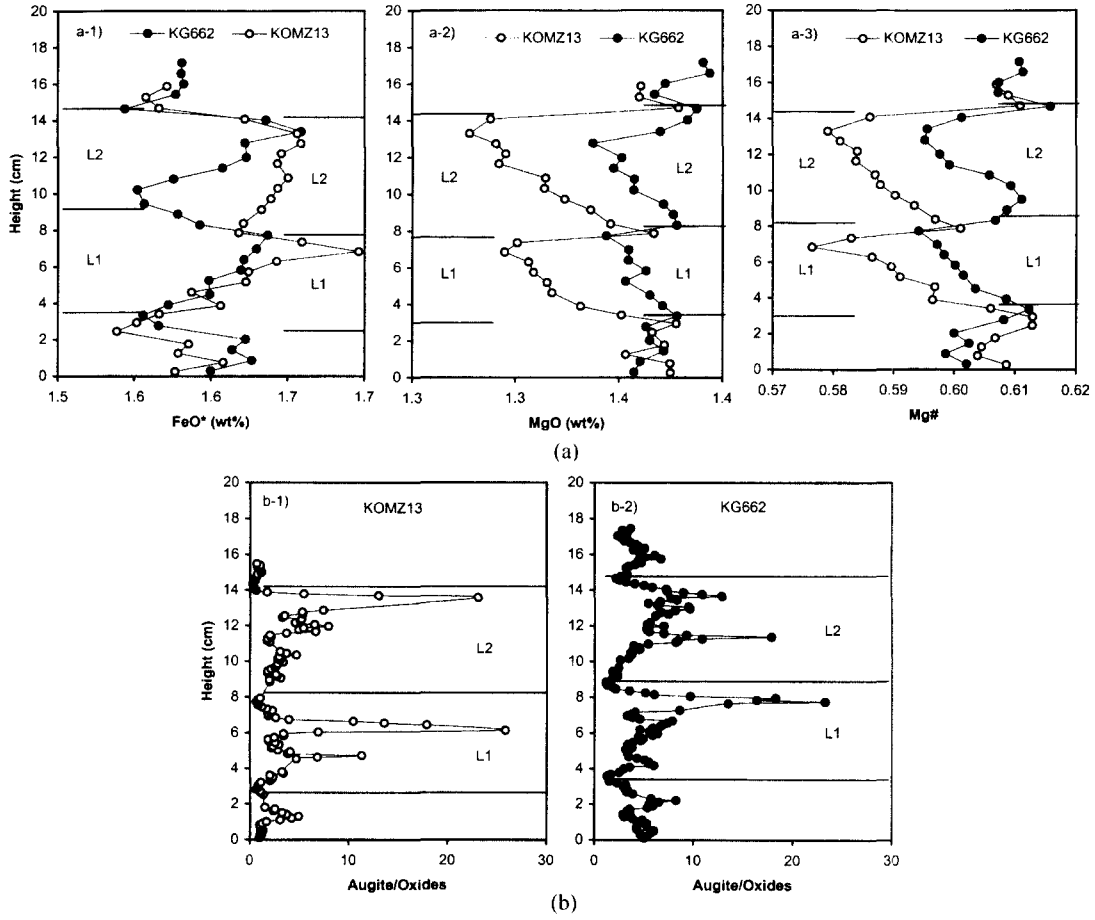

Fig. 4. Compositional variations of pyroxene (a) and the ratio of pyroxene to oxides (b) for two representative sequences of modally-graded layering. Compositional variations of FeO*, MgO and Mg# within individual layers are similar in the two sequences. The most MgO-rich augite occurs at the base of the layers, and does not appear to correlate with pyroxene/oxide or with the abundance of pyroxene

Table 2. Major element analyses of plagioclase separates from two sequences of modally-graded rhythmic layers of the Skaergaard intrusion.

KOMZ13-Plagioclase-rich, modally-graded, rhythmic layer

	Height (cm)	SiO_2	TiO_2	Al_2O_3	Fe_2O_3*	MnO	MgO	CaO	Na_2O	K_2O	P_2O_5	Total
A1	0.3	54.40	0.13	29.48	0.74	<0.01	0.19	9.37	5.89	0.24	0.01	100.45
A2	0.8	54.96	0.13	28.85	0.72	<0.01	0.19	10.10	5.57	0.24	0.01	100.79
A3	1.3	54.84	0.13	28.58	0.71	<0.01	0.19	10.14	5.50	0.24	0.02	100.35
A4	1.8	54.78	0.13	28.84	0.68	<0.01	0.19	10.10	5.65	0.25	0.02	100.65
B1	2.5	55.08	0.13	29.07	0.72	<0.01	0.20	8.96	5.73	0.20	0.01	100.11
B2	2.9	54.64	0.13	29.86	0.71	<0.01	0.20	9.04	5.89	0.22	0.02	100.70
B3	3.4	55.03	0.12	29.46	0.70	<0.01	0.19	9.12	5.83	0.23	0.01	100.72
B4	3.9	54.95	0.12	29.49	0.66	<0.01	0.18	9.08	5.85	0.25	0.02	100.61
C1	4.6	56.03	0.13	28.55	0.64	<0.01	0.18	8.71	5.46	0.25	0.01	99.97
C2	5.2	55.95	0.13	28.75	0.61	<0.01	0.17	8.80	5.63	0.28	0.01	100.35
C3	5.7	56.34	0.13	28.77	0.63	<0.01	0.18	9.09	5.50	0.27	0.01	100.92
C4	6.3	55.85	0.14	27.51	0.67	<0.01	0.16	9.26	5.59	0.28	0.01	99.47
D1	6.8	55.03	0.12	29.63	0.58	<0.01	0.15	8.65	5.90	0.30	0.01	100.39
D2	7.3	55.32	0.12	29.12	0.60	<0.01	0.18	9.17	5.65	0.26	0.02	100.45
D3	7.9	54.95	0.13	29.27	0.61	<0.01	0.18	8.89	5.77	0.22	0.01	100.04
D4	8.4	55.14	0.13	29.43	0.62	<0.01	0.18	9.16	5.74	0.22	0.01	100.65
E1	9.1	56.00	0.12	28.60	0.64	<0.01	0.17	8.73	5.57	0.25	0.01	100.10
E2	9.7	55.69	0.13	28.18	0.68	<0.01	0.18	9.25	5.30	0.23	0.01	99.65
E3	10.3	55.38	0.13	28.74	0.62	<0.01	0.15	8.94	5.59	0.26	0.01	99.83
E4	10.9	55.51	0.12	28.76	0.60	<0.01	0.16	8.92	5.57	0.26	0.01	99.94
F1	11.6	55.24	0.12	29.10	0.59	<0.01	0.14	9.00	5.69	0.26	0.01	100.14
F2	12.2	54.81	0.12	29.21	0.58	<0.01	0.13	9.11	5.70	0.27	0.01	99.95
F3	12.7	56.03	0.12	28.74	0.58	<0.01	0.14	9.52	5.45	0.27	0.01	100.87
F4	13.3	55.26	0.12	29.11	0.59	<0.01	0.13	9.30	5.64	0.28	0.01	100.45
G1	14.1	55.80	0.12	29.24	0.60	<0.01	0.13	8.90	5.73	0.28	0.01	100.82
G2	14.7	55.20	0.13	29.12	0.69	<0.01	0.18	9.16	5.57	0.19	0.01	100.26
G3	15.3	54.98	0.12	29.44	0.64	<0.01	0.15	8.87	5.84	0.21	0.01	100.28
G4	15.9	55.25	0.12	29.30	0.65	<0.01	0.15	9.09	5.72	0.22	0.01	100.52

Fe_2O_3*=total iron as Fe_2O_3

KG662-Pyroxene-rich, modally-graded, rhythmic layer

	Height (cm)	SiO_2	TiO_2	Al_2O_3	Fe_2O_3*	MnO	MgO	CaO	Na_2O	K_2O	P_2O_5	Total
A1	0.3	54.47	0.13	29.97	0.75	<0.01	0.25	9.20	5.69	0.35	0.01	100.84
A2	0.9	54.69	0.13	29.43	0.68	<0.01	0.17	9.32	5.74	0.36	0.02	100.55
A3	1.4	54.56	0.13	29.50	0.65	<0.01	0.16	9.29	5.77	0.40	0.02	100.50
A4	2.0	54.64	0.13	29.09	0.60	<0.01	0.16	9.41	5.65	0.35	0.01	100.05
B1	2.8	55.03	0.13	29.05	0.62	<0.01	0.15	8.75	5.64	0.34	0.01	99.72
B2	3.3	55.14	0.13	28.98	0.68	<0.01	0.17	8.91	5.63	0.36	0.01	100.03
B3	3.9	55.45	0.13	29.12	0.65	<0.01	0.17	9.05	5.67	0.40	0.01	100.66
B4	4.5	55.58	0.13	28.97	0.67	<0.01	0.17	9.01	5.69	0.38	0.01	100.62
C1	5.3	55.56	0.14	28.43	0.68	<0.01	0.16	8.75	5.58	0.35	0.01	99.67
C2	5.8	56.08	0.13	28.55	0.66	<0.01	0.16	8.91	5.61	0.37	0.01	100.51
C3	6.4	55.65	0.13	29.01	0.67	<0.01	0.16	8.92	5.67	0.35	0.01	100.59
C4	7.0	55.43	0.13	29.05	0.61	<0.01	0.15	8.81	5.80	0.35	0.02	100.36
D1	7.7	55.49	0.12	28.94	0.60	<0.01	0.13	8.71	5.93	0.36	0.01	100.31
D2	8.3	55.24	0.12	29.07	0.63	<0.01	0.14	8.87	5.67	0.35	0.01	100.12
D3	8.9	55.24	0.12	28.56	0.61	<0.01	0.16	8.91	5.58	0.34	0.01	99.55
D4	9.5	55.61	0.13	28.86	0.65	<0.01	0.16	9.08	5.65	0.37	0.02	100.52

Table 2. Continued.

KG662-Pyroxene-rich, modally-graded, rhythmic layer

	Height (cm)	SiO_2	TiO_2	Al_2O_3	Fe_2O_3*	MnO	MgO	CaO	Na_2O	K_2O	P_2O_5	Total
E1	10.2	55.52	0.12	28.55	0.61	<0.01	0.14	8.85	5.61	0.33	0.01	99.76
E2	10.8	55.23	0.13	29.03	0.63	<0.01	0.15	9.10	5.72	0.40	0.01	100.41
E3	11.4	55.75	0.13	28.85	0.65	<0.01	0.16	9.17	5.64	0.35	0.01	100.73
E4	12.0	55.48	0.12	28.99	0.61	<0.01	0.15	9.14	5.66	0.35	0.01	100.52
F1	12.8	55.07	0.13	29.45	0.60	<0.01	0.14	8.74	5.77	0.36	0.01	100.29
F2	13.4	55.12	0.12	29.40	0.61	<0.01	0.14	8.90	5.76	0.39	0.01	100.47
F3	14.0	55.31	0.12	29.10	0.60	<0.01	0.15	9.03	5.78	0.39	0.01	100.51
F4	14.6	54.98	0.13	29.15	0.70	<0.01	0.15	9.07	5.68	0.38	0.01	100.25
G1	15.4	54.87	0.13	29.39	0.63	<0.01	0.15	9.05	5.75	0.35	0.01	100.34
G2	16.0	54.93	0.13	29.57	0.65	<0.01	0.16	9.24	5.73	0.35	0.01	100.78
G3	16.6	54.90	0.13	28.87	0.65	<0.01	0.17	9.24	5.65	0.35	0.01	99.99
G4	17.2	54.91	0.13	29.29	0.68	<0.01	0.18	9.20	5.74	0.34	0.02	100.50

Fe_2O_3*=total iron as Fe_2O_3

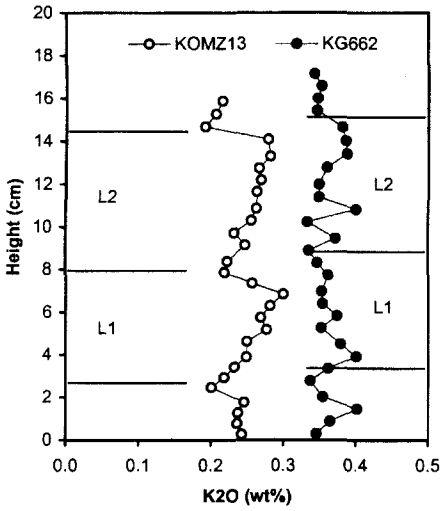

Fig. 5. Compositional variation of K_2O in plagioclase for two representative sequences of modally-graded layering. Note that plagioclase in pyroxene-rich, modally-graded, rhythmic layers is more enriched in K_2O than plagioclase in plagioclase-rich layers, and that plagioclase in plagioclase-rich layers shows systematic variations of K_2O contents with height, which were probably caused by reequilibration between adcumulus overgrowths and the original cumulus grains. The K_2O-rich plagioclase in the pyroxene-rich layers does not appear to have reequilibrated, suggesting that it crystallized in equilibrium with the magma on the floor of the chamber.

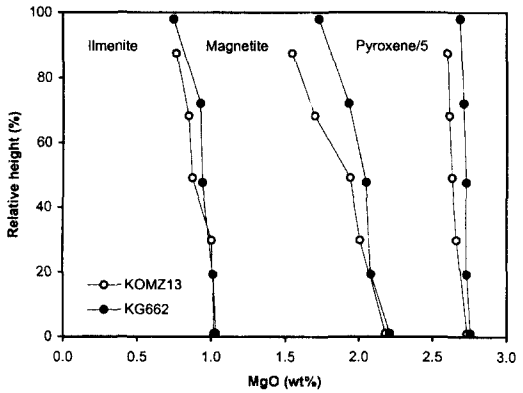

Fig. 6. Interlayer compositional variation of MgO in magnetite, ilmenite, and pyroxene for two representative sequences of modally-graded layering. Compositional variation of MgO in magnetite, ilmenite, and pyroxene within individual layers progressively decreases with height, and is similar in the two sequences.

tents (Table 2). Plagioclase in plagioclase-rich, modally-graded, rhythmic layers is lower in K_2O than plagioclase in pyroxene-rich, modally-graded, rhythmic layers. No significant compositional variation is observed within the layers except for the K_2O contents in plagioclase within the plagioclase-rich layers, which progressively increases with height in each layer (Fig. 5).

5.3. Magnetite and Ilmenite

Magnetite and ilmenite in five sections from a single layer in each sequence were analyzed by electron microprobe (Table 3). Oxides in the two sequences are similar in major element contents, except for MgO (Fig. 6). Both magnetite and ilmenite in the plagioclase-rich, modally-graded, rhythmic layers are lower in MgO than magnetite

Table 3. Electron microprobe analyses of magnetite and ilmenite in two representative layer (L1) from modally-graded rhythmic layers of the Skaergaard intrusion.

Magnetite

	Height (%)	SiO_2	TiO_2	Al_2O_3	Cr_2O_3	FeO*	MnO	MgO	V_2O_5	Total
KOMZ13 D2	94	0.04	16.90	2.13	0.05	76.45	0.33	0.77	2.84	99.51
KOMZ13 C4	74	0.08	15.90	1.84	0.03	78.43	0.31	0.85	2.79	100.24
KOMZ13 C2	52	0.03	16.50	2.11	0.06	78.23	0.32	0.87	2.80	100.92
KOMZ13 B4	27	0.12	16.84	1.84	0.05	77.45	0.37	1.01	2.86	100.54
KOMZ13 B1	1	0.03	17.20	2.09	0.03	76.78	0.39	1.02	2.85	100.38
KG662 D2	98	0.02	16.85	1.58	0.05	77.69	0.38	0.75	2.83	100.15
KG662 C4	78	0.02	16.20	1.93	0.04	78.08	0.34	0.93	2.81	100.35
KG662 C2	54	0.03	17.10	1.72	0.02	77.48	0.41	0.94	2.82	100.52
KG662 B4	25	0.03	15.74	2.09	0.05	77.70	0.38	1.01	2.82	99.82
KG662 B2	1	0.04	17.13	1.82	0.05	77.49	0.39	1.03	2.84	100.79

Ilmenite

	Height (%)	SiO_2	TiO_2	Al_2O_3	Cr_2O_3	FeO*	MnO	MgO	V_2O_5	Total
KOMZ13 D2	94	0.01	50.73	0.04	0.01	46.86	0.47	1.55	0.45	100.12
KOMZ13 C4	74	0.01	51.11	0.04	0.02	47.01	0.48	1.70	0.50	100.87
KOMZ13 C2	52	0.01	50.98	0.04	0.01	46.86	0.47	1.94	0.46	100.76
KOMZ13 B4	27	0.01	50.73	0.04	0.01	46.54	0.47	2.01	0.49	100.30
KOMZ13 B1	1	0.01	50.96	0.05	0.01	46.71	0.49	2.18	0.50	100.91
KG662 D2	98	0.01	50.57	0.04	0.02	47.14	0.49	1.73	0.48	100.47
KG662 C4	78	0.01	51.05	0.04	0.01	46.86	0.47	1.93	0.46	100.83
KG662 C2	54	0.01	50.53	0.04	0.01	47.12	0.50	2.05	0.49	100.73
KG662 B4	25	0.01	51.16	0.03	0.02	46.15	0.49	2.08	0.47	100.42
KG662 B2	1	0.01	50.79	0.04	0.02	46.84	0.49	2.21	0.50	100.89

FeO*=total iron as FeO

Height (%)-Relative height calculated as 0% at bottom and 100% at top of layer.

and ilmenite in the pyroxene-rich, modally-graded, rhythmic layers. No significant compositional variation is observed within either layer for either magnetite or ilmenite, except for the MgO contents, which systematically decrease with height in both magnetite and ilmenite in both analyzed layers (Fig. 6).

6. TRACE ELEMENT GEOCHEMISTRY

6.1. Pyroxene

All 56 pyroxene separates were analyzed for trace elements (Ba, Be, Co, Cr, Cu, Ga, Ni, Sc, Sr, V, Zn, and Zr) by DCP-AES (Table 4). Pyroxene separates from one layer in each sequence were also analyzed for trace elements (Sc, V, Ni, Cu, Zn, Rb, Sr, Y, Zr, Nb, Mo, Cs, Ba, La, Ce, Pr, Nd, Sm, Eu, Gd, Tb, Dy, Ho, Er, Tm, Yb, Lu, Hf, Ta, Pb, Th, and U) by ICP-MS (Table 5). In general, pyroxene separates show similar trace element contents in the two sequences. Pyroxene in the pyroxene-rich, modally-graded, rhythmic layers are richer in Co and Sc than pyroxene in the plagioclase-rich, modally-graded, rhythmic layers. Trace element variations within layers are not as prominent as major element variations in the two sequences. Cu, Zr, Y, and the rare earth elements in plagioclase-rich layers, and Cu in pyroxene-rich layers progressively increase with height in modally-graded layers (Fig. 7). Ni/Co similarly increases with height within layers. Eu/Sm is higher in pyroxene from plagioclase-rich layers than in pyroxene from pyroxene-rich layers.

6.2. Plagioclase

All 56 plagioclase separates from the two sequences of modally-graded, rhythmic layers were analyzed for trace elements (Ba, Be, Co, Cr, Cu, Ni, Sc, Sr, V, Zn, and Zr) by DCP-AES (Table

Table 4. Trace element analyses of pyroxene separates from two sequences of modally-graded rhythmic layers of the Skaergaard intrusion determined by DCP-AES.

KOMZ13-Plagioclase-rich, modally-graded, rhythmic layer

	Height (cm)	Co	Cr	Cu	Ni	Sc	Sr	V	Zn	Zr
A1	0.3	57	7	66	67	98	5	422	116	22
A2	0.8	60	8	70	68	101	4	420	106	23
A3	1.3	57	8	60	67	103	5	420	101	23
A4	1.8	61	8	68	71	106	5	442	111	23
B1	2.5	55	8	77	66	103	4	410	118	22
B2	2.9	58	9	29	69	107	5	424	107	22
B3	3.4	56	12	44	66	107	5	411	108	22
B4	3.9	56	12	49	64	108	5	405	111	22
C1	4.6	57	7	71	70	100	5	439	107	22
C2	5.2	58	9	83	70	103	5	422	116	23
C3	5.7	57	10	90	68	104	4	423	117	23
C4	6.3	57	9	134	72	105	5	422	114	23
D1	6.8	55	9	302	67	101	5	411	140	23
D2	7.3	57	12	111	68	104	5	415	123	23
D3	7.9	58	11	30	68	105	6	418	110	22
D4	8.4	59	12	67	68	106	6	425	106	22
E1	9.1	56	10	94	68	100	4	412	116	22
E2	9.7	57	11	111	67	104	6	418	121	22
E3	10.3	57	10	102	70	103	6	418	118	23
E4	10.9	57	11	105	69	102	5	411	121	23
F1	11.6	54	7	123	65	99	6	413	108	23
F2	12.2	57	11	117	70	101	5	418	122	23
F3	12.7	56	9	126	67	102	5	409	121	23
F4	13.3	55	9	157	66	102	5	408	119	24
G1	14.1	55	7	120	69	98	5	416	120	23
G2	14.7	58	18	51	71	102	5	413	110	22
G3	15.3	55	11	35	67	103	5	416	103	22
G4	15.9	56	8	50	66	102	6	417	102	22

Ba <1; Be <1

KG662-Pyroxene-rich, modally-graded, rhythmic layer

	Height (cm)	Co	Cr	Cu	Ni	Sc	Sr	V	Zn	Zr
A1	0.3	53	14	55	57	104	5	398	111	22
A2	0.9	58	18	59	61	116	6	401	119	23
A3	1.4	64	17	77	65	123	9	417	140	22
A4	2.0	61	20	78	63	123	8	404	120	23
B1	2.8	54	4	79	61	103	5	408	102	22
B2	3.3	58	7	53	64	113	5	421	105	23
B3	3.9	58	8	49	61	105	4	408	108	22
B4	4.5	57	7	64	63	104	4	410	110	22
C1	5.3	56	5	73	62	102	4	417	104	22
C2	5.8	60	8	82	66	109	5	424	110	22
C3	6.4	61	9	85	65	107	5	423	113	22
C4	7.0	64	10	107	69	109	6	428	114	22
D1	7.7	55	4	138	61	101	5	411	117	22
D2	8.3	59	7	56	64	109	6	424	105	22
D3	8.9	56	7	48	62	106	4	418	103	22
D4	9.5	59	8	51	71	106	5	428	120	22

Table 4. Continued

KG662-Pyroxene-rich, modally-graded, rhythmic layer

	Height (cm)	Co	Cr	Cu	Ni	Sc	Sr	V	Zn	Zr
E1	10.2	53	5	69	60	99	6	408	99	22
E2	10.8	58	8	66	65	107	6	420	106	23
E3	11.4	57	9	83	64	106	6	417	107	23
E4	12.0	57	13	91	67	106	6	414	110	22
F1	12.8	57	5	82	63	106	5	421	111	23
F2	13.4	61	8	92	66	110	6	428	110	23
F3	14.0	60	8	81	66	109	5	424	109	23
F4	14.6	59	8	45	63	109	5	422	104	22
G1	15.4	53	7	47	65	103	7	409	100	22
G2	16.0	58	6	56	64	103	4	419	110	23
G3	16.6	59	7	67	67	111	7	430	108	23
G4	17.2	59	10	69	63	110	7	423	94	23

Ba <1; Be <1

6). Plagioclase separates from one layer of each sequence were also analyzed for trace elements (Sc, V, Ni, Cu, Zn, Rb, Sr, Y, Zr, Nb, Mo, Cs, Ba, La, Ce, Pr, Nd, Sm, Eu, Gd, Tb, Dy, Ho, Er, Tm, Yb, Lu, Hf, Ta, Pb, Th, and U) by ICP-MS (Table 7). In general, plagioclase separates show similar trace element contents in the two sequences (Fig. 8). Ba and rare earth elements in plagioclase from plagioclase-rich layers progressively increase with height within the layers. Eu/Sm is lower in plagioclase from plagioclase-rich layers than in plagioclase from pyroxene-rich layers.

7. DISSCUSSION

7.1. Geochemical Variations within Layers

The compositions of the principal minerals of two representative sequences of modally-graded, rhythmic layers show that there are marked variations within individual layers in terms of some major and trace elements (Figs. 4, 5, 6, 7, and 8). Major element variations are observed in K_2O in

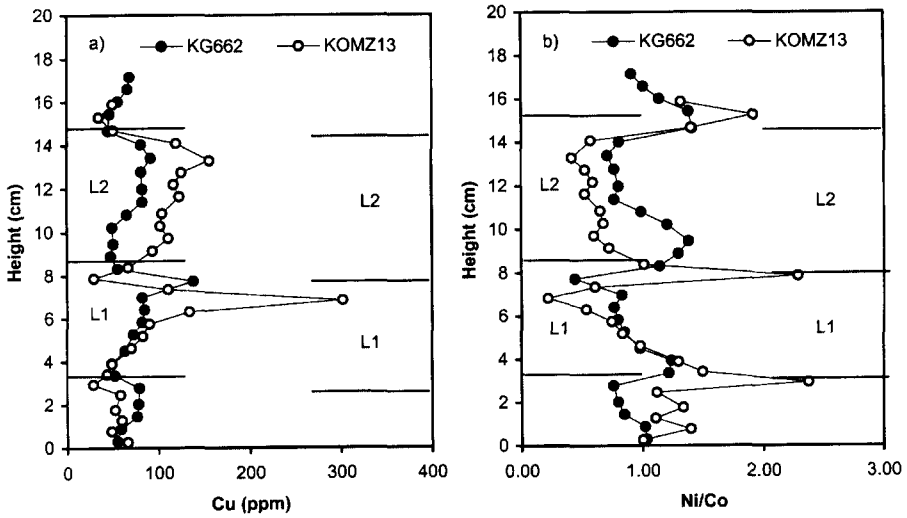

Fig. 7. Interlayer compositional variations of Cu (a) and Ni/Co (b) in pyroxene for two representative sequences of modally-graded layering from the middle zone of the Layered Series. Cu and Ni/Co in pyroxene progressively changes with height in a layer, and are similar in the two sequences.

Table 5. Trace element analyses of plagioclase separates from two sequences of modally-graded rhythmic layers of the Skaergaard intrusion determined by DCP-AES.

KOMZ13-Plagioclase-rich, modally-graded, rhythmic layer

	Height (cm)	Ba	Cu	Sr	V	Zn	Zr
A1	0.3	89	2	560	6	5	4
A2	0.8	96	<1	575	6	4	4
A3	1.3	100	<1	583	7	5	4
A4	1.8	99	<1	578	5	5	4
B1	2.5	78	5	563	6	5	4
B2	2.9	89	6	575	6	5	4
B3	3.4	92	6	566	8	5	4
B4	3.9	98	4	571	4	5	4
C1	4.6	95	2	567	8	5	4
C2	5.2	102	1	576	8	5	4
C3	5.7	104	1	580	7	5	4
C4	6.3	109	3	573	8	5	4
D1	6.8	107	<1	569	4	5	4
D2	7.3	112	<1	575	10	5	4
D3	7.9	89	<1	576	7	5	4
D4	8.4	92	11	579	6	5	4
E1	9.1	92	5	563	7	5	4
E2	9.7	101	5	574	11	5	4
E3	10.3	101	3	573	6	5	4
E4	10.9	102	3	578	5	5	4
F1	11.6	98	2	571	7	4	4
F2	12.2	101	<1	568	10	4	4
F3	12.7	104	1	577	9	4	4
F4	13.3	106	3	575	10	4	4
G1	14.1	109	4	565	6	5	4
G2	14.7	87	4	583	10	5	4
G3	15.3	84	3	578	8	5	4
G4	15.9	91	5	585	8	5	4

Be, Co, Ni, Sc <1

KG662-Pyroxene-rich, modally-graded, rhythmic layer

	Height (cm)	Ba	Cu	Sr	V	Zn	Zr
A1	0.3	92	2	529	10	7	4
A2	0.9	98	2	559	10	6	4
A3	1.4	96	3	559	10	6	4
A4	2.0	98	<1	561	9	5	4
B1	2.8	93	1	543	5	5	4
B2	3.3	97	7	554	6	6	4
B3	3.9	102	2	579	8	5	4
B4	4.5	103	2	579	8	6	4
C1	5.3	100	2	564	8	5	4
C2	5.8	103	1	580	7	5	4
C3	6.4	104	2	581	9	6	4
C4	7.0	102	1	585	9	6	4
D1	7.7	99	1	565	7	5	4

Table 5. Continued.

KG662-Pyroxene-rich, modally-graded, rhythmic layer

	Height (cm)	Ba	Cu	Sr	V	Zn	Zr
D2	8.3	96	5	580	8	6	4
D3	8.9	103	2	579	8	5	4
D4	9.5	104	2	582	12	5	4
E1	10.2	98	1	564	6	5	4
E2	10.8	105	5	580	9	6	4
E3	11.4	106	1	582	10	5	4
E4	12.0	104	1	579	9	5	4
F1	12.8	101	1	556	7	4	4
F2	13.4	101	2	573	9	5	4
F3	14.0	100	1	574	10	5	4
F4	14.6	100	2	577	10	5	4
G1	15.4	99	5	564	6	6	4
G2	16.0	99	2	577	10	5	4
G3	16.6	99	1	576	10	5	4
G4	17.2	98	2	575	11	7	4

Be, Co, Ni, Sc <1

plagioclase, and in MgO and FeO* in pyroxene, ilmenite, and magnetite. Trace element variations are observed for Ba and rare earth elements in plagioclase and for Cu, Zr, Y, and rare earth elements in pyroxene. Similar compositional variations in minerals within individual layers have been previously reported and explained in several different ways (Irvine. 1967; McBirney and Noyes, 1979; Conrad and Naslund, 1989).

Irvine (1967) found a strong positive correlation between the forsterite content of olivine and the modal abundance of olivine and chromite in the rocks of the Muskox intrusion. He attributed this to subsolidus reequilibration between olivine and chromite. Samples with the highest chromite/olivine had the most MgO-rich olivine because recrystallization caused a net transfer of MgO from chromite to olivine. If such a reequilibration model is applicable to the Skaergaard rocks examined in this study containing magnetite and ilmenite rather than chromite and augite rather than olivine, samples with low augite/oxide should contain more MgO-rich augite than samples with high augite/oxide. Although there is a general correlation between augite/oxide and the MgO content in pyroxene, magnetite, and ilmenite, augite/oxide varies considerably within layers, but the MgO contents of the mafic mineral systematically decrease upward in the layers.

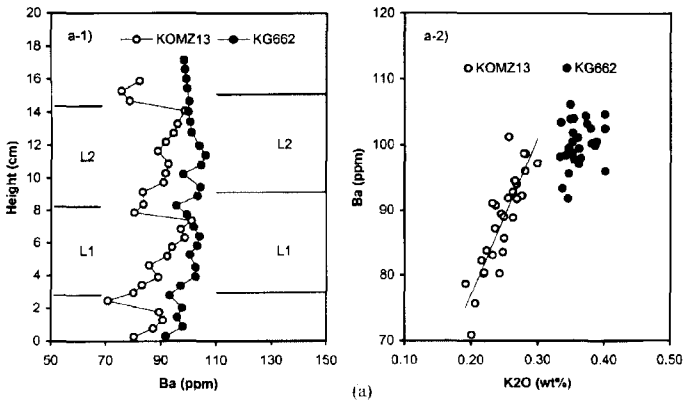

Fig. 8. (a) Compositional variation of Ba in plagioclase plotted versus height (a) and versus K_2O (b) for two representative sequences of modally-graded layering. Note that Ba in plagioclase from plagioclase-rich layers systematically increases within graded layers, which is similar to the K_2O trend. Close correlation between K_2O and Ba suggests that the observed Ba variation was probably also caused by reequilibration between adcumulus overgrowths and the original cumulus grains.

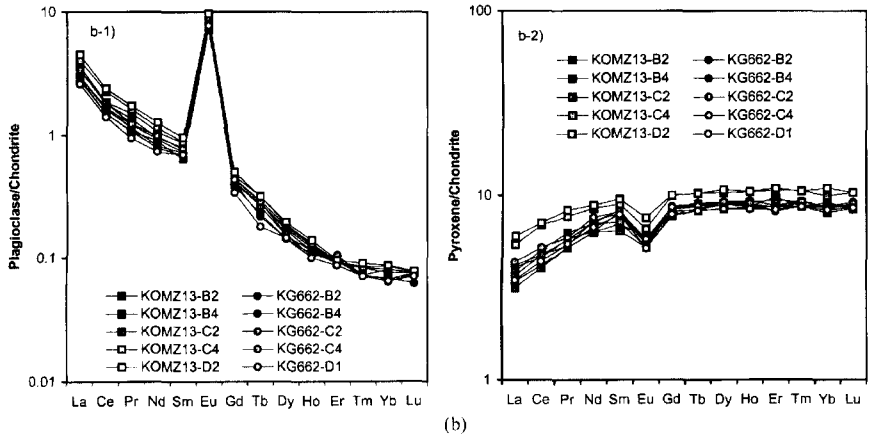

Fig. 8. (b) Chondrite normalized rare earth elements in plagioclase (b-1) and pyroxene (b-2) for two representative sequences of modally-graded layering. Rare earth elements in plagioclase and pyroxene from plagioclase-rich layers systematically increase within graded layers, probably as a result of reequilibration between adcumulus overgrowths and the original cumulus grains.

McBirney and Noyes (1979) analyzed the major mineral phases in a single layer from Upper Zone A. They found that the MgO content in olivine, magnetite, and ilmenite decreased with height within the layer, and suggested that the MgO trend in the minerals was produced by local iron depletion caused by the early crystallization of oxide minerals. Following Wilson and Mathisons model (Wilson and Mathison, 1968) they suggested that oxide minerals nucleate earlier and grow more rapidly than olivine, and thereby, deplete the remaining liquid in iron. If such a model is applicable to the MZ samples in this study, the MgO content of augite should correlate positively with the modal abundance of oxide minerals. Although there is a general upward decrease in both MgO content in augite and oxide abundance, the more detailed intra-layer variations in oxide abundance do not correlate with the augite composition. This model is also dependent upon differences in nucleation rates and, hence, the mode should correlate negatively with grain size, which is not observed.

It has been proposed that reequilibration between adcumulus overgrowths and the original cumulus

Table 6. (a) Trace element analyses of pyroxene and plagioclase separates from representative layers in two sequences of modally-graded rhythmic layers determined by ICP-MS.

Pyroxene

	Height (%)	Sc	V	Ni	Cu	Zn	Rb	Sr	Y	Zr	Nb	Mo	Cs	Ba	Hf	Ta	Pb	Th	U
KOMZ13 D2	94	103	407	71	299	139	0.52	4.5	34.3	24.6	1.71	0.62	0.34	2.7	1.25	0.07	1.42	0.35	0.13
KOMZ13 C4	74	104	418	71	128	124	0.80	4.7	33.7	24.4	1.81	0.52	0.44	2.6	1.13	0.09	1.57	0.27	0.06
KOMZ13 C2	52	100	426	69	79	117	0.35	4.7	30.3	22.6	1.97	0.73	0.37	2.6	0.96	0.06	1.39	0.13	0.03
KOMZ13 B4	27	98	409	67	58	108	0.32	4.6	28.5	21.9	1.62	0.58	0.42	2.5	0.78	0.06	1.55	0.10	0.02
KOMZ13 B2	9	99	410	68	32	103	0.44	4.7	26.7	21.5	2.02	0.55	0.52	2.7	0.84	0.07	1.45	0.57	0.29
KG662 D1	94	104	415	67	140	113	0.86	4.4	26.9	23.0	2.06	0.59	0.47	2.5	0.79	0.07	1.39	0.21	0.07
KG662 C4	78	102	420	69	88	114	1.18	5.1	29.4	22.7	1.74	0.78	0.42	2.6	0.90	0.07	1.18	0.37	0.15
KG662 C2	54	100	419	68	76	111	1.52	4.9	28.8	23.3	2.21	0.63	0.39	2.6	0.96	0.07	1.59	0.93	0.55
KG662 B4	25	97	413	67	68	114	0.89	4.4	27.8	21.6	1.61	0.51	0.41	2.5	0.76	0.08	1.58	0.22	0.07
KG662 B2	1	106	420	70	51	103	0.80	5.5	30.0	22.1	1.47	0.54	0.49	2.7	0.74	0.05	1.51	0.13	0.03

Height (%)-Relative height calculated as 0% at bottom and 100% at top of layer.

Plagioclase

	Height (%)	Sc	V	Ni	Cu	Zn	Rb	Sr	Y	Zr	Nb	Mo	Cs	Ba	Hf	Ta	Pb	Th	U
KOMZ13 D2	94	0.21	8.4	3.5	4.1	5.1	2.2	594	0.51	3.2	1.72	0.79	0.05	105	0.08	0.03	0.01	0.01	0.09
KOMZ13 C4	74	0.18	6.0	3.6	3.6	5.3	3.1	599	0.55	3.3	1.72	0.83	0.04	98	0.09	0.04	0.01	0.03	0.20
KOMZ13 C2	52	0.21	6.0	3.6	3.9	5.5	2.4	603	0.52	3.3	1.84	0.73	0.03	96	0.08	0.03	0.01	0.04	0.17
KOMZ13 B4	27	0.19	6.7	3.5	4.0	5.4	1.6	592	0.46	3.3	2.00	0.85	0.03	91	0.10	0.05	0.01	0.05	0.32
KOMZ13 B2	9	0.21	8.7	3.7	4.3	5.3	5.2	569	0.45	3.5	2.59	0.83	0.04	84	0.11	0.03	0.01	0.05	0.29
KG662 D1	94	0.20	4.4	3.7	3.2	5.0	2.5	569	0.39	3.3	1.44	0.73	0.04	95	0.11	0.03	0.01	0.07	0.21
KG662 C4	78	0.23	9.8	4.6	3.3	5.3	3.9	659	0.66	3.0	1.57	0.88	0.05	113	0.12	0.03	0.01	0.07	0.33
KG662 C2	54	0.241	0.1	4.5	3.4	5.5	3.5	661	0.56	2.9	1.54	0.97	0.05	115	0.08	0.03	0.01	0.05	0.20
KG662 B4	25	0.25	9.1	4.6	3.8	5.2	3.0	637	0.44	2.9	1.52	0.85	0.04	112	0.13	0.04	0.01	0.02	0.16
KG662 B2	1	0.23	6.1	3.9	4.4	5.5	2.8	597	0.41	2.8	1.51	0.88	0.04	104	0.09	0.04	0.01	0.02	0.21

Height (%)-Relative height calculated as 0% at bottom and 100% at top of layer.

Table 6. (b) Rare earth element analyses of pyroxene and plagioclase separates from representative layers in two sequences of modally-graded rhythmic layers determined by ICP-MS.

Pyroxene

	Height (%)	La	Ce	Pr	Nd	Sm	Eu	Gd	Tb	Dy	Ho	Er	Tm	Yb	Lu
KOMZ13 D2	94	4.22	12.9	2.31	12.0	4.22	1.26	5.92	1.10	7.88	1.71	5.20	0.77	2.72	0.76
KOMZ13 C4	74	3.82	12.6	2.13	11.6	3.97	1.10	5.87	1.11	7.58	1.69	5.09	0.78	2.47	0.76
KOMZ13 C2	52	2.72	9.25	1.74	9.58	3.16	0.88	4.98	0.97	6.65	1.49	4.48	0.68	2.18	0.65
KOMZ13 B4	27	2.23	7.36	1.44	8.58	2.83	0.87	4.56	0.89	6.20	1.40	4.14	0.64	1.99	0.62
KOMZ13 B2	9	2.41	7.62	1.44	8.62	3.09	0.99	4.59	0.90	6.58	1.41	4.65	0.64	2.28	0.61
KG662 D1	94	2.45	8.01	1.51	9.14	3.47	0.86	4.67	0.89	6.18	1.37	3.98	0.64	2.07	0.63
KG662 C4	78	3.08	9.52	1.64	10.3	3.61	0.97	5.10	0.94	6.76	1.47	3.89	0.68	2.11	0.66
KG662 C2	54	2.59	8.62	1.60	9.68	3.69	0.92	4.94	0.94	6.53	1.45	4.11	0.67	2.16	0.65
KG662 B4	25	2.95	8.64	1.48	9.91	3.53	0.91	4.80	0.90	6.75	1.42	3.90	0.64	2.15	0.64
KG662 B2	1	2.88	8.40	1.61	8.71	3.58	0.94	5.13	0.98	6.76	1.51	4.19	0.68	2.16	0.67

Height (%)-Relative height calculated as 0% at bottom and 100% at top of layer.

Table 6. (b) Continued.

Plagioclase

	Height (%)	La	Ce	Pr	Nd	Sm	Eu	Gd	Tb	Dy	Ho	Er	Tm	Yb	Lu
KOMZ13 D2	94	3.20	4.39	0.48	1.74	0.43	1.62	0.30	0.03	0.14	0.02	0.05	0.01	0.02	0.01
KOMZ13 C4	74	2.86	4.16	0.45	1.59	0.39	1.53	0.28	0.03	0.14	0.02	0.04	0.01	0.02	0.01
KOMZ13 C2	52	2.58	3.39	0.42	1.47	0.39	1.46	0.27	0.03	0.13	0.02	0.04	0.01	0.02	0.01
KOMZ13 B4	27	2.13	3.07	0.34	1.28	0.33	1.24	0.25	0.03	0.13	0.02	0.04	0.01	0.02	0.01
KOMZ13 B2	9	1.97	2.76	0.30	1.24	0.29	1.21	0.24	0.03	0.12	0.02	0.04	0.01	0.02	0.01
KG662 D1	94	1.84	2.57	0.26	1.01	0.31	1.30	0.20	0.02	0.11	0.02	0.04	0.01	0.02	0.01
KG662 C4	78	2.38	3.36	0.34	1.36	0.34	1.51	0.26	0.03	0.11	0.02	0.05	0.01	0.02	0.01
KG662 C2	54	2.40	3.32	0.37	1.32	0.35	1.50	0.25	0.03	0.11	0.02	0.05	0.01	0.02	0.01
KG662 B4	25	2.12	2.97	0.32	1.13	0.32	1.44	0.24	0.02	0.10	0.02	0.04	0.01	0.02	0.01
KG662 B2	1	2.04	2.74	0.30	1.09	0.31	1.34	0.23	0.02	0.11	0.02	0.04	0.01	0.02	0.00

Height (%)-Relative height calculated as 0% at bottom and 100% at top of layer.

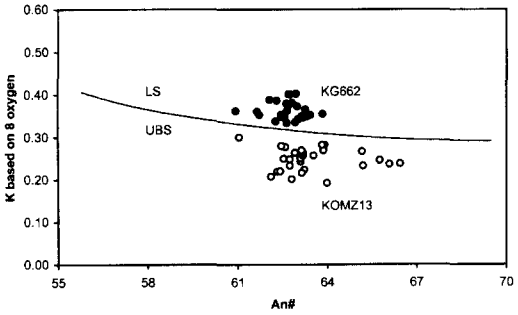

Fig. 9. A plot of K versus An# for plagioclase of the Skaergaard intrusion. Plagioclase from the plagioclase-rich macro layer is systematically lower in K_2O than plagioclase from the pyroxene-rich macro layer. The only pronounced difference in major element composition between LS plagioclase and UBS plagioclase is that, in spite of the fact that the UBS is in general richer in K_2O than the LS, plagioclase in the LS has more K_2O than plagioclase in the UBS (Naslund, 1984). Plagioclase in the plagioclase-rich, macro-rhythmic layers has K_2O contents similar to those of UBS plagioclase suggesting that these layers have accumulated plagioclase transported from the roof zone of the intrusion

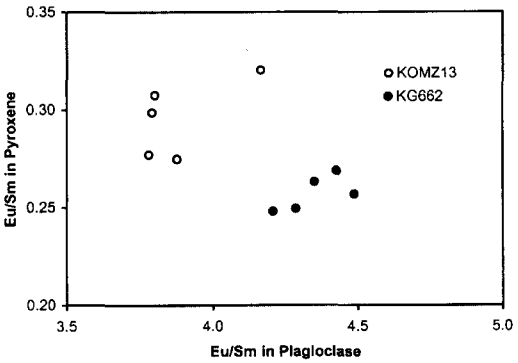

Fig. 10. Eu/Sm in pyroxene separates and plagioclase separates. Open symbols are from a plagioclase-rich macro layer, and filled symbols are from a pyroxene-rich macro layer.

grains could also lead to variations in the chemical composition of certain mafic minerals in areas where the modal abundances of the minerals vary considerably (Barnes, 1986; Chalokwu and Grant, 1987). In this model, the composition of a mineral should correlate positively with its modal abundance assuming a uniform distribution of adcumulus material. Conrad and Naslund (1989) suggested that MgO variation in olivine in rhythmic layers from UZa and LZc of the Skaergaard intrusion was caused by reequilibration between adcumulus overgrowths and the original cumulus grains because the olivine composition within the layers correlates strongly with the modal abundance of olivine, but not with the abundance of oxide minerals or with the ratio of oxide minerals to olivine. If such a model is applicable to the augite, ilmenite, and magnetite compositions of the MZ samples examined in this study, the most MgO-rich composition of each phase should occur where the phase is most abundant, as is observed for ilmenite and magnetite. The composition of augite, however, is more strongly correlated with its position in an individual layer than with the abundance of pyroxene. Reequilibration with an iron-rich interstitial liquid percolating downward

from the top of each layer, would cause more reequilibration in the upper part of a layer and less near the base, as is observed. Alternatively, if the post-deposition porosity increases upward in the layer, reequilibration with interstitial iron-rich melts would more strongly affect the top of the layer than the base.

In the layers examined in this study, plagioclase in plagioclase-rich, modally-graded, rhythmic layers shows systematic variations in K_2O, Ba, and rare earth element contents with height. Subsolidus reequilibration between mineral phases can be ruled out because there are no other K_2O, Ba, or rare earth element-rich phases in the samples. A nucleation dependent process could produce compositional variations in plagioclase, but this process can also be ruled out by the strong positive correlation between mode and grain size of plagioclase within each layer (Fig. 3). It has been previously reported that there are no systematic K_2O variations in the cores of the plagioclase within modally-graded layers from UZa and LZc (McBirney and Noyes, 1979; Conrad and Naslund, 1989), and that zoning structures are common in Skaergaard plagioclase (Carr, 1954; Maaloe, 1976). Plagioclase separates in this study, however, represent mixtures of original cumulus cores and later formed adcumulus rims overgrown from trapped liquid with a high K_2O and excluded trace element content. The K_2O and some of the trace element variations in the plagioclase separates, therefore, appear to be best explained by reequilibration between adcumulus overgrowths and the original cumulus grains. A model in which early formed crystals reequilibrated with an interstitial liquid percolating downward through the layer fits well with the observed data. Close correlation between K_2O and Ba suggests that the observed Ba variation was probably caused by a similar process (Fig. 8). Reequilibration is only observed in the plagioclase-rich, macro-rhythmic layers that contain plagioclase that was initially low in K_2O, and hence, out of equilibrium with the interstitial melt. The pyroxene-rich, macro-rhythmic layers contain plagioclase with a higher initial K_2O content that was in equilibrium with the interstitial melt, and, hence, did not reequilibrate.

The results discussed above suggest that there were no compositional variations in the initial cumulus compositions of the silicate phases within individual modally-graded layers. There were, however, initial compositional differences between plagioclase in the plagioclase-rich, macro-rhythmic layers and plagioclase in the pyroxene-rich, macro-rhythmic layers, which were only partly removed by later reequilibration.

7.2. Origin of modally-graded rhythmic layers

Although numerous theories have been proposed for the origin of igneous layering structures (c.f. Naslund and McBirney, 1996), the three mechanisms most commonly proposed for modally-graded, rhythmic layers are: nucleation-controlled processes, gravity-controlled processes, and flow segregation in magma currents.

Variations between nucleation rates and growth rates in supersaturated systems have been proposed as a layer-forming mechanism for modally-graded, rhythmic layering in the Skaergaard intrusion (Maaloe, 1978). In this model, supersaturation develops until one phase nucleates, after which growth of the nucleated phase decreases supersaturation and, hence, the nucleation rate of that phase, and increases supersaturation and, hence, the nucleation rate of the other phases. As a given phase nucleates and grows it causes a compositional shift in the magma under relatively isothermal conditions that results in the nucleation and growth of additional phases. As this mechanism depends upon differences in nucleation rates to cause differences in modal abundances, layers with greater abundances of a phase should have more nuclei and, hence, a smaller average grain size than layers with lower abundances and fewer nuclei. Samples from layered sequences in which modal layering has been formed by differences in nucleation rates, should therefore, demonstrate a negative correlation between mode and average grain size for individual phases. Direct measurements of average grain sizes in two sequences of modally-graded, rhythmic layers (Fig. 3) suggest that there is a positive correlation between mode and grain size. Similar results have been reported for modally-grained, rhythmic layers in the lower zone and upper zone of the Skaergaard layered series (Conrad and Naslund, 1989). These results suggest that variations in nucleation rate did not play an important role in the formation of the mod-

ally-graded, rhythmic layering examined for this study.

Wager and Deer (1939) proposed that modally-graded layers were produced by the settling of mineral phases with different densities under the influence of gravity. In theory, crystals in magma will settle according to the well-known Stokes law equation. Magma is a non-Newtonian liquid, however, so before crystals can begin to settle, the downward force on a crystal must overcome the yield strength of the magma. Experimental studies and field measurements on lava flows (Shaw *et al.*, 1968; Murase and McBirney, 1973; McBirney and Murase, 1984) indicate that yield strengths are too high to initiate the settling of the major mineral phases in normal basaltic magma. In a stagnant magma with yield strength between 500 and 1000 dynes per cm^2 (typical of a basic magma), olivine and pyroxene crystals would have to attain a size of 3 to 5 cm in order to overcome the yield strength and initiate settling (McBirney and Noyes, 1979). The yield strength of magma is greatly decreased during viscous flow, however, suggesting that crystal settling may be more effective in moving magmas. An additional problem with a crystal settling mechanism is that plagioclase was less dense than the Skaergaard magma (McBirney and Noyes, 1979), and would therefore, have been more likely to float, or remain neutrally buoyant in the magma than to settle.

Graded layers formed by crystal settling should be graded in terms of both mineral density and grain size, with the densest minerals and the largest grain sizes concentrated at the base of each layer. In the Skaergaard intrusion graded layers are generally density sorted, but as described above, the largest grain sizes are not concentrated at the bases of individual layers. This result, combined with the calculated yield strength and density of the Skaergaard magma (McBirney and Noyes, 1979), suggests that gravity settling alone was probably not responsible for the formation of the modally-graded, rhythmic layering examined in this study.

Numerous sedimentary-like structures including scour-and-fill structures, slumping, mineral imbrications, and angular unconformities are closely associated with modally-graded layers in the Skaergaard intrusion (Wager and Brown, 1967; Irvine, 1974, 1987; Conrad and Naslund, 1989) and are quite prominent in the middle zone sequence examined in this study. The yield strength of magma is greatly decreased during viscous flow (McBirney and Noyes, 1979) and, hence, crystals in moving magmas may overcome the yield strength to settle down to the floor. Modally-graded layers have been attributed to crystal-rich, density currents that broke away from the walls of the intrusion and moved out across the floor leaving a density-sorted layer behind (Wager and Brown, 1967; Irvine, 1987; Conrad and Naslund, 1989). The presence of discontinuities in the wall and roof sequences makes this interpretation likely. The material in the layer may have been derived primarily from the current (Wager and Brown, 1967; Irvine, 1987) or may have a substantial contribution from a stagnant zone of in situ crystallization on the floor that was stirred and sorted by the passing current (Conrad and Naslund, 1989). Density sorting in stagnant liquids or in laminar flow should result in grain-size sorting in which the largest grains of each mineral occur at the base of the layer, while grain-size sorting in a turbulent flow (elutriation) should result in the largest grains of each mineral occurring where that mineral is most abundant. Although the Skaergaard modally-graded layers do not show obvious size sorting, the positive correlation between mode and grain size in detailed studies (Conrad and Naslund, 1989; this report) suggest that modally-graded layers have formed by flow segregation in magma currents during turbulent flow.

7.3. Origin of macro-rhythmic layers

Layering in the Middle Zone of the Skaergaard intrusion is characterized by alternating plagioclase-rich and pyroxene-rich layers with sharp upper and lower boundaries, that range in thickness from 0.3 to 0.6 m and can be traced in outcrop for 2 km or more along strike with little obvious change in thickness (Naslund *et al.*, 1991). The modally-graded, rhythmic layers described above are contained within these macro-rhythmic layers, and are abundant in both plagioclase-rich and pyroxene-rich macro layers. In some sections, however, both the plagioclase-rich and pyroxene-rich macro layers contain no modally-graded internal layering. Their abrupt upper and lower con-

tacts, their uniform thicknesses across the entire intrusion, their lack of any apparent relationship to local sedimentary-like structures, and their apparently random thicknesses, suggest that the macro-rhythmic layers are formed by an irregular process that can be turned on and off, and that simultaneously affects the entire magma chamber. Although the layering is difficult to follow on the outcrop, individual layers can be easily distinguished from a distance and appear to cross the entire intrusion. It was originally proposed (Naslund *et al.*, 1991) that the plagioclase-rich layers form during periods of stagnation, and that the pyroxene-rich layers form during periods of convection. The mineral proportions in the pyroxene-rich layers, however, more closely approximately cotectic abundances than do the proportions in the plagioclase-rich layers. The only pronounced difference in major element composition between LS plagioclase and UBS plagioclase is that, in spite of the fact that the UBS is, in general, richer in K_2O than the LS, plagioclase in the LS has more K_2O than plagioclase in the UBS (Naslund, 1984). K_2O solubility in plagioclase is significantly reduced as P_{H2O} increases (Franco and Schairer, 1951; Yoder *et al.*, 1957). Naslund (1984) suggested that the volatile (water) content in the UBS magma was higher than that in the LS magma and hence, reduced the solubility of K_2O in UBS plagioclase. Increased P_{H2O} would also be expected to lower the crystallization temperature of the UBS, but might not effect the An content of the crystallizing plagioclase owing to the competing effects of temperature and P_{H2O}. If UBS plagioclase crystallized at an average temperatures 20°C lower than that of LS plagioclase, the UBS plagioclase would be 2.5% poorer in An. If, however, the P_{H2O} in the UBS is 0.5 kbar higher than in the LS, the An content in UBS plagioclase should be 2 to 4% richer in An. The effects of temperature and P_{H2O} on An content of plagioclase, therefore, would tend to cancel one another (Naslund, 1980; Jang and Naslund, 2001). Plagioclase in the plagioclase-rich, macro-rhythmic layers has K_2O contents similar to those of UBS plagioclase, suggesting that these layers have accumulated plagioclase transported from the roof zone of the intrusion (Fig. 9). If such is the case, the plagioclase-rich layers may have formed during periods of convection, while the pyroxene-rich layers formed during periods of stagnation. The relatively sharp layer boundaries, the variable layer thicknesses, and the intrusion-wide extent of individual layers, suggest a mechanism that is randomly and abruptly turned on and off. A model based on periodic convection and non-convection fits well with these observations. Similar interpretations have been proposed as mechanisms for rhythmic layer formation in the Stillwater intrusion (Hess, 1960) and Ilimaussaq intrusion (Engell, 1973).

Naslund (1980) reported that UBS plagioclase has lower Eu/Sm than does LS plagioclase, and attributed the difference to more oxidizing conditions at the roof of the intrusion. Plagioclase in the plagioclase-rich, macro-rhythmic layers has lower Eu/Sm than plagioclase in the pyroxene-rich, macro-rhythmic layers (Fig. 10) suggesting that the plagioclase-rich layers may have accumulated extra roof zone plagioclase. Pyroxene in the plagioclase-rich macro layers has higher Eu/Sm than does pyroxene in the pyroxene-rich macro layers, confirming that the plagioclase in the plagioclase-rich layers was not locally crystallized. If plagioclase had crystallized in situ in the plagioclase-rich layers, both plagioclase and pyroxene should have lower Eu/Sm owing to increased depletion of Eu in the magma by the crystallization of excess plagioclase. The addition of plagioclase to the plagioclase-rich macro layers increased the bulk Eu/Sm in the layer, resulting in higher Eu/Sm in pyroxene which crystallized primarily in situ.

7.4. Implications of intermittent convection on iron enrichment differentiation trends

If intermittent convection in the Skaergaard magma chamber results in the precipitation of excess plagioclase in the LS, it could have a significant influence on the development of silica-enrichment and iron-enrichment in the Skaergaard magma. Wager (1960) proposed a differentiation model for the Skaergaard intrusion in which iron is enriched in the magma during crystallization, and silica remains at a relatively constant level until very late in the crystallization history. An iron-enrichment differentiation trend has been assumed by many subsequent investigators (McBirney, 1975, 1989; Naslund, 1984; Hoover, 1989; McBir-

ney and Naslund, 1990; Morse, 1990; Brooks *et al.*, 1991; Tegner, 1997). A silica-enrichment, iron-depletion trend for the Skaergaard magma has been proposed (Hunter and Sparks, 1987; 1990) based in part on phase equilibria and the removal of minerals from the magma in cotectic proportions. If convection in the magma chamber results in the selective reabsorption of pyroxene and magnetite relative to plagioclase and ilmenite, and the concentration of excess plagioclase and ilmenite in the LS, this process will act to inhibit silica-enrichment and iron-depletion and will result in the removal of minerals from the magma in non-cotectic proportions.

8. CONCLUSIONS

1. Systematic compositional variations within individual modally-graded layers were observed for both major and trace elements. The K_2O variation in the plagioclase separates from the plagioclase-rich, macro-rhythmic layers appear to be best explained by K_2O poor cores overgrown by K_2O-rich adcumulus rims. MgO and FeO* variations in pyroxene, ilmenite, and magnetite appear to be the result of subsolidus reequilibration between early-formed mafic minerals and an interstitial iron-rich magma. In both cases, the degree of reequilibration appears to be more strongly correlated with position in the layer than with individual mineral abundances or any mineral abun-dance ratios, suggesting reequilibration with interstitial liquid percolating downward from the top of the layer to the base. There does not appear to be any original chemical variations in the cumulus compositions of individual minerals within graded layers.

2. Modally-graded, rhythmic layers in the middle zone of the Layered Series occur within thicker plagioclase-rich and pyroxene-rich, macro-rhythmic layers. Within both plagioclase-rich and pyroxene-rich, macro-rhythmic layers, plagioclase is concentrated at the top of modally-graded layers and the oxide minerals are concentrated at the base of modally-graded layers. The maximum grain sizes of plagioclase and oxides occur at the same level in the layer as their maximum modal abundances. Modally-graded layers appear to have formed by a mechanism that is independent of that which formed the macro-rhythmic layers. Indeed, macro-rhythmic layers occur both with and without internal, modally-graded layers. The mineral compositions within the modally-graded layers are, in general, identical to the minerals in unlayered host rock. The most likely mechanism for the formation of these modally-graded layers involves local density currents moving down the walls of the intrusion and across the floor resulting in a flow segregation of crystals growing in situ on the floor of the intrusion.

3. Plagioclase in the plagioclase-rich, macro-rhythmic layers has a lower K_2O content lower than plagioclase in pyroxene-rich, macro-rhythmic layers. Plagioclase compositions in the plagioclase-rich, macro-rhythmic layers are similar to those of the UBS, suggesting that these layers have accumulated excess plagioclase transported from the roof zone of the intrusion. The plagioclase-rich, macro-rhythmic layers may have formed during periods of convection, while the pyroxene-rich, macro-rhythmic layers formed during periods of stagnation. Convection within the Skaergaard magma chamber appears to have resulted in a plagioclase-rich crystal assemblage at the base of the convection cells. Owing to the higher temperatures and lower water contents of the magma at the floor of the intrusion, crystal-rich magma transported from the roof of the intrusion to the floor undergoes selective resorption in which pyroxene and oxides are selectively remelted and plagioclase is concentrated in the remaining crystal assemblage. The higher ilmenite/magnetite in the plagioclase-rich, macro-rhythmic layers compared to pyroxene-rich, macro-rhythmic layers suggests that magnetite may be selectively resorbed relative to ilmenite as magma moves from the roof to the floor of the chamber.

ACKNOWLEDGEMENT

The author wishes to thank Dr. Dick Naslund for his thoughtful guidance and stimulating discussion in improving this paper, and Dr. Joe Graney for his help with ICP-MS analyses and Mr. Bill Blackburn for his help with Electron microprobe analyses. This work was supported in part by a Korea Government Scholarship to YDJ, and NSF grant EAR8804936 to HRN.

REFERENCES

Barnes S.J (1986) The effect of trapped liquid crystallization on cumulus mineral composition in layered intrusions. Contrib. Mineral. Petrol., v. 93, p. 524-531.

Bence A.E, Albee A.L (1968) Empirical correction factors for the electron microanalysis of silicate oxides. J. Geol., v. 76, p. 382-403.

Boudreau A.E, McBirney A.R (1997) The Skaergaard Layered Series. Part III. Non-dynamic layering. J. Petrol., v. 38, p. 1003-1020.

Brooks C.K, Larsen L.M, Nielsen T.F.D (1991) Importance of iron-rich tholeiitic magmas at divergent plate margins: a reappraisal. Geology, v. 19, p. 269-272.

Carr, J.M (1954) Zoned plagioclase in layered gabbros of the Skaergaard intrusion, East Greenland. Mineral. Mag., v. 30, p. 367-375.

Chalokwu G.I, Grant N.K (1987) Re-equilibration of olivine with trapped liquid in the Duluth complex, Montana. Geology. v. 15, p. 71-74.

Conrad M.E, Naslund H.R (1989) Modally-graded rhythmic layering in the Skaergaard intrusion. J. Petrol., v. 30, p. 251-269.

Engell J. (1973) A closed system crystal-fractionation model for the agpaitic Ilimaussaq intrusion, South Greenland, with special reference to the lujavrites. Bull Geol. Soc. Denmark., v. 22, p. 334-362.

Feigenson M.D, Carr M.J (1985) Determination of major, trace, and rare-earth elements in rocks by DCP-AES. Chem. Geol., v. 51, p. 19-27.

Franco R.R, Schairer J.F (1951) Liquidus temperatures in mixtures of the feldspars of soda, potash, and lime. J. Geol., v. 59, p. 259-267.

Govindaraju K (1994) 1994 compilation of working values and sample description for 383 geostandards. Geostand. Newsl., v. 18, p. 1-158.

Hess H.H (1960) Stillwater igneous complex. Mem Geol Soc. Am., v. 80, p. 1-230.

Hoover J.D (1989) Petrology of the Marginal Border Series of the Skaergaard intrusion. J. Petrol., v. 30, p. 399-439.

Hunter RH, Sparks RSJ (1987) The differentiation of the Skaergaard intrusion. Contrib. Mineral. Petrol., v. 95, p. 451-461.

Hunter R.H, Sparks R.S.J (1990) A reply to comments on The differentiation of the Skaergaard intrusion. Contrib. Mineral. Petrol., v. 104, p. 248-254.

Hutchinson C.S (1974) Laboratory Handbooks of Petrographic Techniques. John Wiley and Sons, New York, p. 1-527.

Irvine T.N (1967) Chromian spinel as a petrographic indicator: Part II Petrologic applications. Can. J. Earth Sci., v. 4, p. 71-103.

Irvine T.N (1974) Petrology of Duke Island ultramafic complex, southeastern Alaska. Mem. Geol. Soc. Am., v. 138, p. 1-240.

Irvine T.N (1987) Layering and related structures in the Duke Island and Skaergaard intrusions: similarities, differences, and origins. In: Parsons, I. (ed.) Origins of Igneous Layering. Reidel, Dodrecht, p. 185-245.

Irvine T.N, Anderson J.C.O, Brooks C.K (1998) Included blocks (and blocks within blocks) in the Skaergaard intrusion: Geologic relations and the origins of rhythmic modally graded layers. Bull. Geol. Soc. Am., v. 110, p. 1398-1447.

Jang Y.D, Naslund H.R (2001) Major and Trace Element Composition of Skaergaard Plagioclase; Geochemical Evidence for Changes in Magma Dynamics During the Final Stage of Crystallization of the Skaergaard Intrusion. Contrib. Mineral. Petrol., v. 140, p. 441-457.

Maaloe S. (1976) The zoned plagioclase of the Skaergaard intrusion, East Greenland. J. Petrol., v. 17, p. 398-419.

Maaloe S (1978) The origin of rhythmic layering. Mineral. Mag., v. 42, p. 337-345.

McBirney A.R (1975) Differentiation of the Skaergaard intrusion. Nature (London), v. 253, p.691-694.

McBirney A.R (1989) The Skaergaard Layered Series: I Structure and average compositions. J. Petro., v. 1 30, p. 363-397.

McBirney A.R, Naslund H.R (1990) The differentiation of the Skaergaard intrusion-a discussion. Contrib. Mineral. Petrol., v. 104, p. 235-247.

McBirney A.R, Nicolas A (1997) The Skaergaard Layered Series: II Magmatic flow and dynamic layering. J. Petrol., v. 38, p.569-580.

McBirney A.R, Noyes R.M (1979) Crystallization and layering of the Skaergaard intrusion. J. Petrol., v. 20, p. 487-554.

McBirney A.R, Murase T. (1984) Rheological properties of magmas. Ann. Rev. Earth Planet. Sci., v. 12, p. 337-357.

Morse S.A (1990) The differentiation of the Skaergaard intrusion. Contrib. Mineral. Petrol., v. 104, p. 240-244.

Murase T, McBirney A.R (1973) Properties of some common igneous rocks and their melts at high temperatures. Geol. Soc. Am. Bull., v. 84, p. 3563-3592.

Naslund H.R (1980) Part I Petrology of the Upper Border Group of the Skaergaard intrusion, East Greenland; and Part II An experimental study of liquid immiscibility in iron-bearing silicate melts. PhD dissertation, Univ Oregon, USA, p. 1-347.

Naslund H.R (1984) Petrology of the Upper Border Series of the Skaergaard intrusion. J. Petrol., v. 25, p. 185-212

Naslund H.R, McBirney AR (1996) Mechanisms of formation of igneous layering. In: Layered Intrusion R G Cawthorn (ed) Elsevier Science, Amsterdam, p. 1-43.

Naslund H.R, Turner P.A, Keith D.W (1991) Crystallization and layer formation in the middle zone of the Skaergaard intrusion. Bull. Geol. Soc. Denmark, v. 38, p. 165-171.

Shaw H.R, Peck D.L, Wright T.L, Okamura R. (1968) The viscosity of basaltic magma: an analysis of field measurements in Makaopuhi lava lake, Hawaii. Am. J. Sci., v. 266, p. 225-264.

Tegner C. (1997) Iron in plagioclase as a monitor of the differentiation of the Skaergaard intrusion. Contrib. Mineral. Petrol., v. 128, p. 45-51.

Vincent E.A, Phillips R (1954) Iron-Titanium oxide minerals in layered gabbros of the Skaergaard intrusion, East Greenland, Part I. Chemistry and ore-microscopy. Geochim. Cosmochim. Acta, v. 6, p. 1-26.

Vincent E.T (1960) Ulvospinel in the Skaergaard intrusion, East Greenland. N Jb Mineral Abh Bd, v. 94, p. 993-1016.

Wager L.R (1960) The major element variation of the Layered Series of the Skaergaard intrusion and a re-esti-

mation of the average composition of the hidden Layered Series and of the successive residual magma. J. Petrol., v. 1, p. 364-398.
Wager L.R, Brown G.M (1967) Layered Igneous Rocks. W. H. Freeman and Co., San Francisco, p. 1-588.
Wager L.R, Deer W.A (1939) (re-issued 1962) Geological Investigations in East Greenland, Part III. The Petrology of the Skaergaard Intrusion Kangerdlugssuaq, East Greenland. Medd om Groenland, v. 105, p. 1-352.
Wilson N.M, Mathison C.I (1968) The Eulogie Park gabbro, a layered basic intrusion from eastern Queensland. J. Geol. Soc. Australia, v. 15, p. 139-146.
Yoder H.S Jr, Stewart D.B, Smith J.R (1957) Ternary feldspars. Yb Carnegie Instn Wash, v. 56, p. 206-214.

2001년 8월 31일 원고접수, 2001년 12월 19일 게재승인.